European Journal of Medicinal Chemistry 77 (2014) 166–175

Contents lists available at ScienceDirect

European Journal of Medicinal Chemistry

journal homepage: http://www.elsevier.com/locate/ejmech

Original article

Design, synthesis & evaluation of condensed 2*H*-4-arylaminopyrimidines as novel antifungal agents

Kishor S. Jain [a,*], Vijay M. Khedkar [b], Nikhilesh Arya [a], Prasad V. Rane [c], Pratip K. Chaskar [d], Evans C. Coutinho [b]

[a] Department of Pharmaceutical Chemistry, Sinhgad Institute of Pharmaceutical Sciences, Lonavala, Pune, 410401 Maharashtra, India
[b] Department of Pharmaceutical Chemistry, Bombay College of Pharmacy, Kalina, Mumbai, 400098 Maharashtra, India
[c] Department of Pharmaceutical Chemistry, RJSPM's College of Pharmacy, Moshi-Alandi Road, Pune, 412105 Maharashtra, India
[d] Department of Pharmaceutical Chemistry, Vivekanand Education Society's College of Pharmacy, Chembur, Mumbai, 400074 Maharashtra, India

ARTICLE INFO

Article history:
Received 15 December 2013
Received in revised form
21 February 2014
Accepted 28 February 2014
Available online 3 March 2014

Keywords:
Antifungal activity
Condensed pyrimidines
Docking
Lanosterol 14-α-demethylase
MWI
SAR

ABSTRACT

A small, focussed library of condensed 2*H*-4-arylaminopyrimidines, with 3-diversity points, based on an initial design by molecular docking study of this scaffold at the active site of the fungal enzyme of cytochrome P_{450} family, lanosterol 14α-demethylase (CYP51) was synthesized through a one-pot green chemical synthetic protocol. The screening of the synthesised compounds for antifungal activity against *Candida albicans*, *Aspergillus fumigatus* & *Aspergillus niger* revealed activity in many of the compounds as comparable to that of fluconazole. Based on the antifungal activity and physicochemical property data of these derivatives, a meaningful SAR has been proposed.

1. Introduction

In recent years, the incidence and severity of life threatening fungal infections have increased, particularly in patients with impaired or compromised immunity [1], signifying the urgent need for development of new alternative antifungal agents [2]. Of the various invasive mycotic infections in humans, majority are caused by *Candida* and *Aspergillus* species, of which *Candida albicans* is one of the main causes of nosocomial fungal infectious diseases. The other species, *Aspergillus fumigatus* has become one of the most prevalent airborne fungal pathogens [3]. Presently, the most widely employed drugs like amphotericin B and the azole class of antifungals suffer from drawbacks. While, the former has poor pharmacokinetics and potential for toxicity, the resistance development by the fungal strains against the later has become rampant [4,5]. These reasons highlight the urgent need for the discovery of newer antifungal drugs, particularly bearing nonconventional chemical structures and which are effective and safe [6]. It is well known that the azoles exert their activity through the inhibition of the fungal enzyme, lanosterol 14α-demethylase (CYP51). This enzyme is a member of the cytochrome P_{450} super family and is implicated in the biosynthesis of fungal ergosterol, by catalyzing the oxidative removal of the 14α-methyl group of lanosterol to give the $\Delta^{14,15}$-unsaturated key intermediates [7]. Recent studies have shown that typical azole inhibitors fit in the putative active site of CYP51 by a combination of heme co-ordination, hydrogen bonding, π–π stacking and hydrophobic interactions [8]. It is reported that in the active site of CYP51 the 1,2,4-triazole ring of the antifungal azole is positioned perpendicularly to the porphyrin plane with a ring nitrogen atom (N_4 of 1,2,4-triazole) coordinated to the heme iron of CYP51. This co-ordination is of key importance for the antifungal activity. The halogenated phenyl group sits deep in the same hydrophobic binding cleft in the active site of the target enzyme CYP51. These interactions of azoles at the active site of CYP51, provide the basis for the design of novel *N*-heterocyclic derivatives as potential antifungal agents with a broad antifungal spectrum and possibly with less potential to develop drug resistance.

Condensed pyrimidine ring system exhibits wide range of biological activities [9]. We have reported some condensed pyrimidine derivatives, as novel lipid lowering agents (**I**) [10–13], proton pump inhibitors (**II**) [14], and anti-proliferative agents (**III**) [15].

* Corresponding author.
E-mail address: drkishorsjain@gmail.com (K.S. Jain).

http://dx.doi.org/10.1016/j.ejmech.2014.02.066
0223-5234/

Considerable anti-proliferative and anti-tumour activity potential observed in condensed 2*H*-4-(substituted-phenyl)amino-pyrimidines **III** [15], prompted us to think of exploring this scaffold also, for antifungal activity. This thinking had two reasons;

1. The urgent need for search of novel structures bearing antifungal activity, due to increase in resistance to the existing azole drugs by fungal strains &
2. This scaffold though new for antifungal activity, combines the nitrogen heterocyclic system; pyrimidine & its aromatic amine side chain, which could afford better binding at the CYP51 active site (Fig. 1).

Herein, we report the design of a novel series of condensed 2*H*-4-substitutedanilino-pyrimidines based on the molecular docking studies of a few derivatives, its microwave irradiation (MWI) based one-pot synthesis and its evaluation for antifungal activity. The antifungal activity data and physicochemical properties have been utilized to delineate some optimal structural information for the activity.

2. Results and discussion

2.1. Chemistry

The synthetic protocol involves the MWI assisted transformation of a variety of *o*-amino ester substrates, involving their cyclocondensation and further chlorination with formamide-$POCl_3$ mixture and subsequent nucleophilic displacement reaction with appropriate substituted aniline, to afford the corresponding condensed 2*H*-pyrimidin-4-arylamines (**1**–**6**), in around 30–60 min, in excellent yields and purity (Scheme 1) [16]. This novel synthetic protocol under MWI is a one pot multicomponent reaction which is high yielding, eco-friendly, rapid, novel as well as, eliminating intermittent workups. Initially, six compounds, **1a**–**6a**, were synthesized and evaluated. Thereafter, based on the observations, the synthesis of remaining derivatives was undertaken.

2.2. Antifungal study

The *in vitro* antifungal activities of the compounds **1a**–**6a** were determined by using the serial micro dilution method in 96 multicell microlitre plates in duplicate, in culture media comprising of potato pulp: 200 g/l, dextrose: 20 g/l and agar: 25 g/l adopting the reported procedures [17,18]. The minimum inhibitory concentrations (MIC) values (μg/ml) were obtained from triplicate assay (three of two test tubes with identical results were taken as MIC's) against *C. albicans* (ATCC® 90028), *A. fumigatus* (ATCC® 204305) and *Aspergillus niger* (ATCC® 9142). These MIC values are represented in Tables 1 and 2 and compared with fluconazole, as well as, docking scores of some of these compounds.

2.3. Docking study

A perusal of the geometries of fluconazole and the 2*H*-4-(4-fluorophenylamino)-pyrazolo[3,4-*d*]pyrimidine (**1a**), reveals spatial differences in their overlap (Fig. 2) and thus, indicating the possibility of involvement of different sets of amino acid residues at the active site of the fungal CYP51 during their interactions. This opens up a possibility of evolving a new scaffold with less propensity to resistance development by the fungal strains to it.

Indeed a comparison between the docking modes of fluconazole and these inhibitors (**1a** & **1b**) at the active site of CYP51 (Figs. 3–5), revealed some promise for the envisaged structures. Like the N-4 atom of the 1,2,4-triazole ring of fluconazole, the N-3 of the condensed pyrimidin-4-amines, is also bound to the heme iron. Similarly, like the difluorophenyl moiety of fluconazole, the substituted-phenyl ring of the arylamino moiety of the condensed pyrimidin-4-amine, seems to be involved in hydrophobic interactions with a set of amino acids in close vicinity. Few of these amino acids are common to both fluconazole and the ligands. This can be explained on the basis of difference in the 3D geometries of fluconazole and these ligands as discussed above. Further, these compounds have an amino functionality for additional interactions in the CYP51 activity. The interaction of the pyrazole ring fused to the pyrimidine also which cannot be overlooked.

The receptor (active site of CYP51) interaction maps for fluconazole and representative condensed 2*H*-4-arylaminopyrimidines (**1a** & **1b**) are depicted in Figs. 3–5, while the interaction data (*Glide score, Glide energy and amino acids of active site involved*), as well as, antifungal activity data are given in Table 1.

The docking scores of these compounds (**1a** & **1b**) were nearly comparable to that of fluconazole and interestingly their antifungal activities against three resistant fungal strains were better than fluconazole (Table 1).

Interestingly, when three more derivatives **1c**, **1d** & **1e** were synthesized and evaluated for their antifungal activity against same three different pathogenic fungal strains, all of them were found to exhibit better antifungal activities than the drug. The rank order of activity being **1c** ≥ **1a** ≥ **1b** > **1d** > **1e**, indicating the influence of the electron withdrawing groups present on the arylamino ring of these compounds.

Analysis of the Glide docking scores showed that these compounds docked to the active site of the cytochrome P_{450} sterol 14α-demethylase in a manner comparable to that of fluconazole

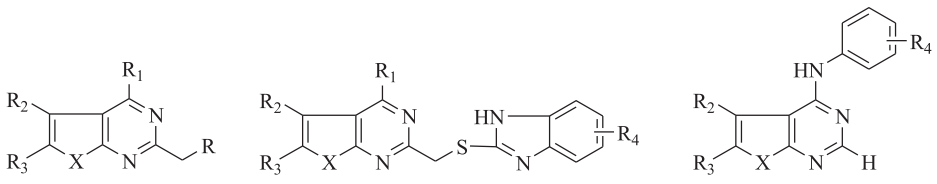

R = Electron withrawing groups;
R_1= OH, Halo, NH_2 ;
R_2, R_3 = Alkyl, aryl, cycloalkyl, H, carboxyalkyl etc.;
X = S, O, N-, -HC=CH-, -N-N=, HC=N- ;
R_4 = H, halo, alkoxy etc.

Fig. 1. Bioactive condensed pyrimidines.

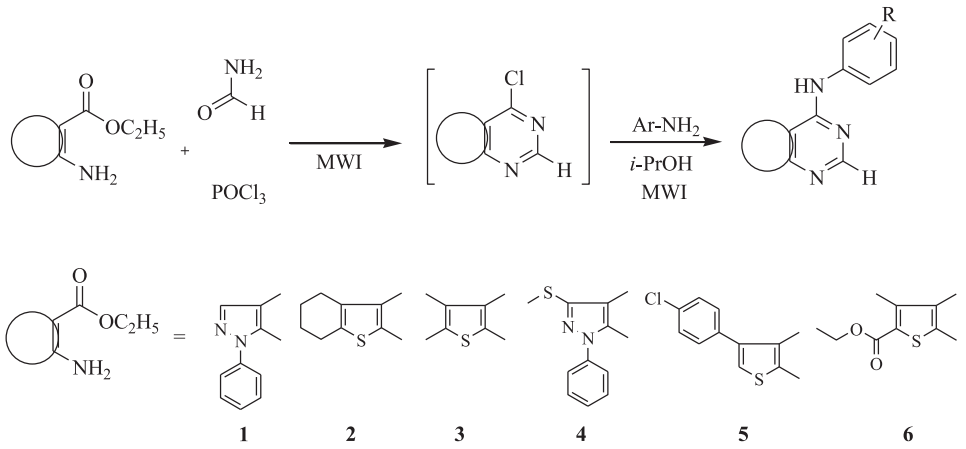

Scheme 1. Synthetic protocol for target compounds (**1a**–**6a**).

(Table 1). Thus, the antifungal activity of these ligands is reflected by their interaction with the heme atom as well as amino acids in the CYP51 active site, where the pyrimidine ring & the arylamino side chain; comprising of the amino moiety, aryl ring and its substituent, all play very important roles. Furthermore, the interaction of these ligands at the active site of CYP51 may also be influenced by the heterocyclic ring fused to the 2*H*-4-arylaminopyrimidine scaffold along with the substituents borne by it. Therefore, to study the effect of this fused ring along with its substituents, some more docking experiments were performed with more varied condensed 2*H*-4-arylaminopyrimidines, followed by their actual synthesis and antifungal evaluation. The correlation of the docking and antifungal activity data could lead to fruitful information. Thus, compounds **2a**, **3a**, **4a**, **5a** & **6a** were designed and studied for their docking interactions and synthesized and evaluated for their antifungal activity (Table 2) (Figs. 6–10).

All the seven compounds **1a, 1b, 2a, 3a, 4a, 5a** & **6a**, as well as fluconazole, were analyzed for their docking modes in the active site of the enzyme. Although the real interaction profile for the synthesized compounds discussed herein has not been resolved experimentally, it is interesting to discuss the predicted interactions for the best docking poses. Six out of these seven compounds (except **5a**) exhibit better activity as well as glide scores as compared to that of fluconazole.

The active site of cytochrome P_{450} sterol 14α-demethylase is highly conserved and there are many amino acid residues in it, participating in close van der Waals and coulombic interactions with the inhibitor, when bound to it. Detailed analysis of the per-residue interaction between the synthesized compounds and the enzyme in comparison with fluconazole revealed some key interactions that appear to play a role in the binding of these molecules to the target.

All the ligands were found coordinated to the iron of the heme group present in the active site to more or less extent. This is a very important observation pointing to the fact, that the pyrimidine derivatives may share the same inhibition mechanism as fluconazole which is also coordinated with the metal ion in the enzyme active site. However, this interaction could not be quantified because of the coordinating nature of the interaction and the lack of terms for quantifying metal–ligand complexes. Also, it is not always the pyrimidine ring N_3 atom being involved in the interaction with the heme iron, but also the side chain NH, the 'S' of methylthio

Table 1
Molecular docking data and antifungal data of compounds (**1a**–**e**).

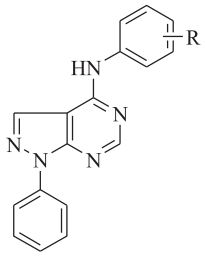

Compd. no.	R	Glide score	Glide energy (kcal/mole)	E_{vdw} (kcal/mole)	$E_{elect.}$ (kcal/mole)	mMIC[a]		
						Candida albicans	*Aspergillus niger*	*Aspergillus fumigatus*
1a	4-F	−8.14	−48.923	−36.629	−12.294	0.0011	0.0026	0.0012
1b	4-Cl	−6.81	−34.835	−36.289	02.041	0.0024	0.0012	0.0013
Fluconazole		−7.34	−52.922	−33.765	−19.156	0.0075	0.0075	0.0040
1c	3-Cl, 4-F	[b]	[b]	[b]	[b]	0.0011	0.0010	0.0012
1d	4-Br	[b]	[b]	[b]	[b]	0.0028	0.0022	0.0022
1e	H	[b]	[b]	[b]	[b]	0.0045	0.0024	0.0028

[a] Molar minimum inhibitory concentration.
[b] Docking experiments not performed for this compounds.

Table 2
Molecular docking data and antifungal data of compounds (**1a**–**6a**).

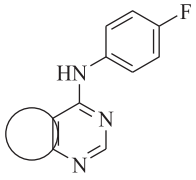

Sr. No.		Glide score (rank order)	Glide energy (kcal/mole)	E_{vdw} (kcal/mole)	$E_{elect.}$ (kcal/mole)	mMIC			Sum of rank orders (overall rank order for activity)
						Candida albicans	*Aspergillus niger*	*Aspergillus fumigatus*	
						(Rank order for activity)			
1	**2**	**3**	**4**	**5**	**6**	**7**	**8**	**9**	**10**
2a	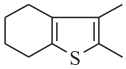	−8.28 (**4**)	−47.751	−37.058	−10.693	0.0013 (**3**)	0.0105 (**5**)	0.0105 (**6**)	14 (**5**)
3a	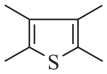	−9.04 (**1**)	−46.787	−31.855	−14.931	0.0005 (**1**)	0.0029 (**4**)	0.0015 (**3**)	08 (**2**)
4a	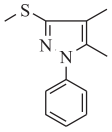	−8.57 (**3**)	−37.397	−27.381	−10.016	0.0031 (**4**)	0.0023 (**2**)	0.0024 (**4**)	10 (**4**)
5a	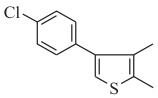	−6.33 (**6**)	−20.895	−19.080	−01.814	0.0081 (**5**)	0.0351 (**6**)	0.0045 (**5**)	16 (**6**)
6a	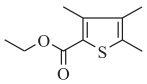	−8.68 (**2**)	−46.557	−32.543	−14.014	0.0094 (**6**)	0.0005 (**1**)	0.0005 (**1**)	08 (**2**)
1a	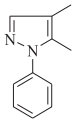	−8.14 (**5**)	−48.923	−36.629	−12.294	0.0011 (**2**)	0.0026 (**3**)	0.0012 (**2**)	07 (**1**)

The rank orders in columns 7–9 are the antifungal activity rank orders for the compounds against corresponding fungal strain indicated under respective columns.
The overall rank orders in column 10 are given after considering the overall antifungal activity of the individual compounds against all 3 fungal strains.
Compound **3a** is ranked 2; equal to compound **6a** in antifungal activity. Thus, rank order is **1a ≥ 3a ≥6a > 4a > 2a > 5a**.

substituents are seen involved in some of the cases. Thus, the target compounds could be predicted to bind with the heme, but with different affinities. A perusal of the data in Tables 2 and 3 as well as the docking poses in Figs. 3–10, reveal that in case of compounds **1a**, **2a**, **3a, 4a** and **6a**, either the pyrimidine N_3 atom or the side chain NH– are involved in binding with the heme iron, though the later is bit at a distance than N_3. Also the phenyl ring is also oriented close to the heme for hydrophobic interactions. In case of compound, **5a**, both the N_3 atom & the side chain NH are little farther, so their interaction with heme iron seems to be comparatively, weaker. In case of **4a**, it is the side chain 'NH–' and the 'S' of methylthio substituent are seem to be involved in this interaction. In case of compound **1b**, only N_3 is oriented close for interaction with the heme iron. Therefore, the interaction of these ligands with the amino acids was also studied. A different set of amino acids of the CYP51 active site are involved in the interactions with the ligands as compared to those with fluconazole. Only MET-123 & ALA-110 are common, as far as the sets of amino acids in close vicinity (~5.0 Å from the molecular surface of ligands) to the difluorophenyl group of fluconazole & the 4-fluorophenyl group of the arylamino moiety of the condensed pyrimidin-4-amines (**1a**–**6a**) are concerned. The amino acid TYR-116 is most prominently involved in the interaction in case of all ligands.

These interactions together, contribute to the docking energies and docking scores of these ligands. In case of **5a**, the lower glide score (docking score −5.95) and possibly its overall lower antifungal activity can be attributed to the steric hindrance of the 4-chlorophenyl ring attached to its thiophene moiety, causing the compound to adopt a different conformation in the active site of CYP51 wherein both, its pyrimidine N_3 as well as side chain NH are a bit drifted away from the heme iron and thus, the interaction at heme is reduced considerably.

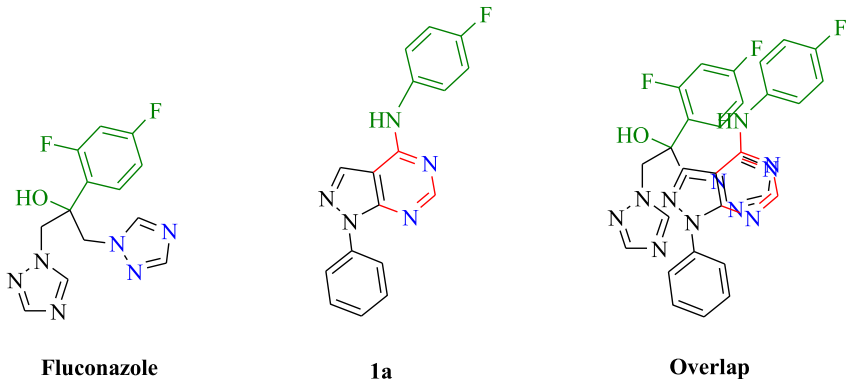

Fig. 2. Overlap of Fluconazole with condensed 2*H*-4-(4-fluorophenylamino)pyrazolo-pyrimidine: Difference in spatial geometries.

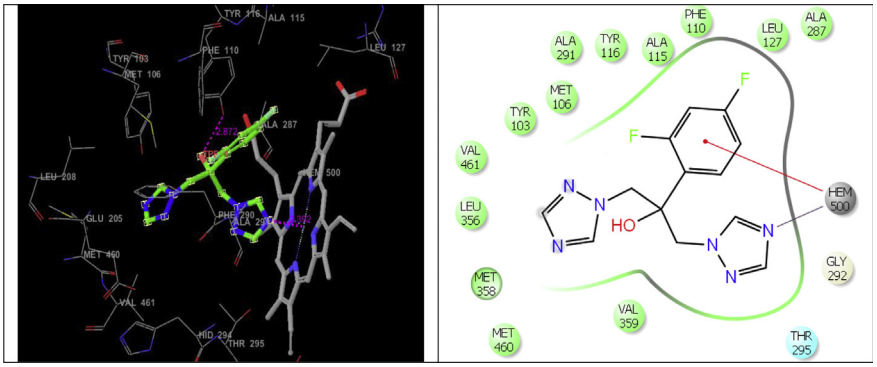

Fig. 3. Docking mode of Fluconazole in the active site of CACYP51.

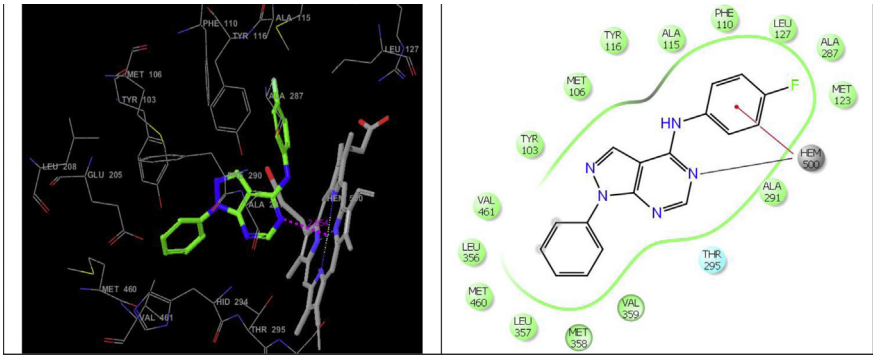

Fig. 4. Docking mode of Compound **1a** in the active site of CACYP51.

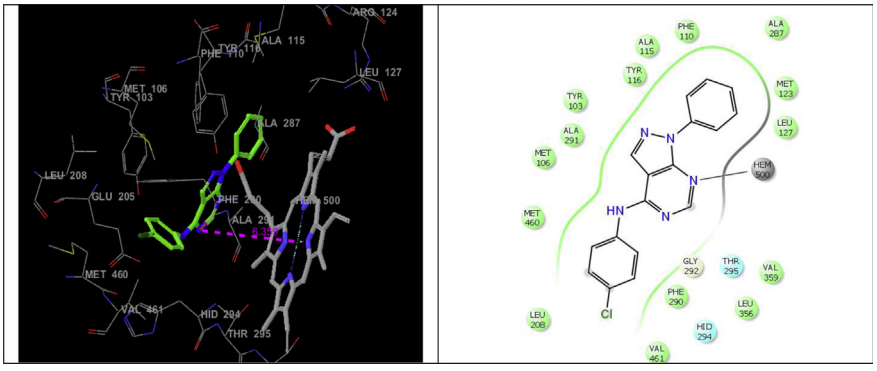

Fig. 5. Docking mode of Compound **1b** in the active site of CACYP51.

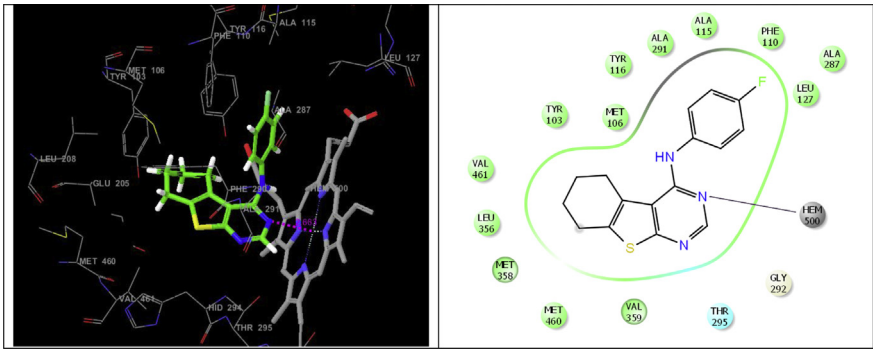

Fig. 6. Docking mode of compound **2a** in the active site of CACYP51.

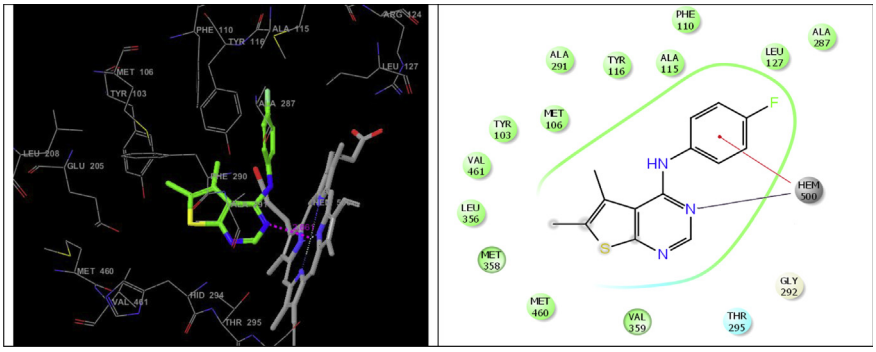

Fig. 7. Docking mode of compound **3a** in the active site of CACYP51.

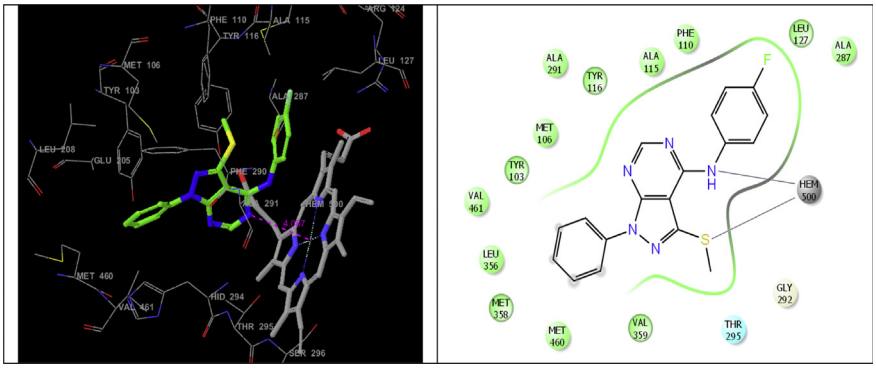

Fig. 8. Docking mode of compound **4a** in the active site of CACYP51.

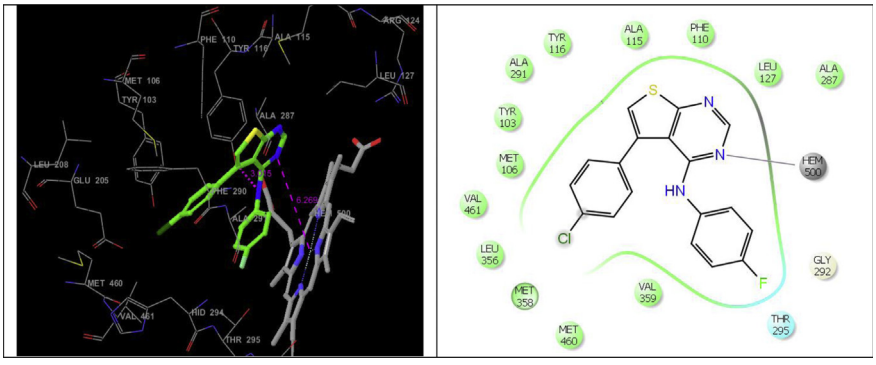

Fig. 9. Docking mode of compound **5a** in the active site of CACYP51.

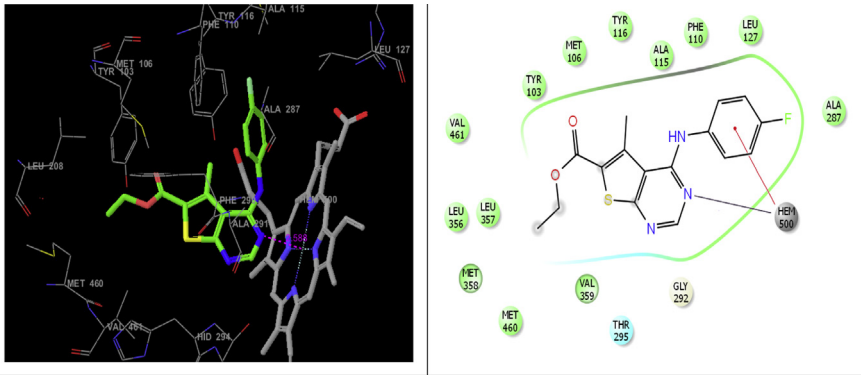

Fig. 10. Docking mode of compound **6a** in the active site of CACYP51.

On other hand, though the pyrimidine N_3 of **4a** is also distanced away from the heme iron, this is compensated by the close proximity of the arylamino side chain NH and the corresponding 'S' of the methylthio substituent groups of this ligand to the heme iron. In case of **6a**, the carbonyl –C=O of the ester group is closely involved in the interaction with the amino acids, MET-106, TYR-103 and TYR-116. These interactions may be leading to better docking scores and antifungal activities of these compounds.

On careful examination of the docking interactions of the three most active of these compounds; **1a**, **3a**, and **6a** as compared with those of fluconazole at the enzyme active site, few important things are evident as described in Table 3.

Compounds **1a**, **3a** and **6a** showed relatively stronger electrostatic interactions fairly comparable to that of fluconazole, which could possibly also contribute to their good glide scores and antifungal activities. Compound **6a** has poorer E_{vdw}, E_{elect} as well as glide scores & predictably lesser antifungal activity as compared to fluconazole.

Rank order for the compounds with respect to their docking scores, −9.04 (**3a**) > −8.68 (**6a**) > −8.57 (**4a**) > −8.28 (**2a**) > −8.14 (**1a**) > −6.33 (**5a**).

Interestingly, when a systematic analysis of the antifungal activity data (mMIC values) of these ligands against the three different fungal strains was done by assigning them rank orders (see foot note for Table 2), it is found that the rank order for the overall antifungal activity is as follows; **1a** ≥ **3a** ≥ **6a** > **4a** > **2a** > **5a**.

This is not in agreement with the rank order for the docking scores for these compounds mainly due to compound **1a**, which though lower in rank docking score, is considerably higher ranked in the antifungal activity.

A plausible explanation for this change of rank order in actually observed overall antifungal activity seems to indicate the role of some other structural feature or property prominently influencing the interaction at the CYP51 active site. Interestingly, a consideration on the nature of the ring fusion at the pyrimidine addresses this anomaly in the correlation of docking scores *vs* antifungal activity, within the series to some extent. The lipophilicity of the ring fused to the pyrimidine seems to influence the overall antifungal activity of the compounds, inversely (Table 4). The compounds **1a**, **3a**, **4a** & **5a** all have the rings fused to the pyrimidine scaffold with lower ClogP values in range of 2.68–3.76; while the compounds **2a** & **5a** carry more lipophilic rings with ClogP, 4.308 & 5.05, respectively.

Close analysis of the results and discussions above lead to the conclusion for the following key structure–activity relationship (SAR) points (Fig. 11):

3. Conclusions

Thus, a new scaffold has been proposed for potential antifungal activity. The structural difference of these compounds from the azoles can make them less prone to the development of resistance by pathogenic fungal strain against them. The good docking scores as well as antifungal activity of these compounds have been justified by investigating their interaction at the active site of CYP51. A meaningful SAR has been developed.

4. Experimental

4.1. General

Melting points were determined using a Veego electronic melting point apparatus model MP-D containing silicon oil bath with stirrer and are uncorrected. The purity of the synthesized compounds was tested using precoated TLC plates (silica gel 60 F_{254} plates, Merck) and visualization was achieved via UV light absorption. The IR absorption spectra were recorded on Perkin Elmer Spectrum, BX II FTIR spectrometer, using (KBr) pellets and absorption frequencies (n) are stated in cm^{-1}. The ^1H NMR spectra ($CDCl_3$) were measured on Varian Mercury 300 MHz spectrometer. The chemical shifts are expressed in parts per million (δ ppm). Tetramethylsilane (TMS) was used as an internal standard. The LC-ESI/MS analysis was carried out on LCQ-Advantage (Thermo Finnigan, San Jose, CA, USA) ion trap mass spectrometer. Microwave synthesizer (Questron Technologies Corp., Canada; model-ProM) having monomode open vessel was used for the synthesis. Elemental analyses for compounds were obtained using a Flash EA 1112 Thermofinnigan Instrument.

4.2. General procedure for synthesis of condensed 2H-pyrimidin-4-amines (*1a–6a* and *1b–e*)

All the compounds (**1a–6a** and **1b–e**) were prepared by taking respective *o*-aminoesters and appropriate substituted anilines as per the procedure reported earlier by us [16] (Yield 80–92%).

4.2.1. N-(4-Fluorophenyl)-1-phenyl-1H-pyrazolo[3,4-d]pyrimidin-4-amine (*1a*)

Yield: 82.35%; mp 174–176 °C; IR (KBr): 3301 (N–H), 2365 (C–H), 1584 (N=N), 975 (C–F) cm^{-1}; ^1H NMR (300 MHz, $CDCl_3$) δ ppm: 7.2–7.8 (m, 4H, NH–Ar–*H*), 8.2–8.4 (s, 5H, N–Ar–*H*), 8.6 (s, 1H, N–N=C*H* at 5), 9.2 (s, 1H, N=C*H*–N at 2), 10.1 (s, 1H, N*H* at 4); ESI-MS *m/z*: 306 (M+1), 212, 195, 112. *Anal.* Calcd. for $C_{17}H_{12}FN_5$ (305.31): C, 66.88; H, 3.96; N, 22.94. Found: C, 66.74; H, 3.86; N, 22.82.

Table 3
Comparison of interactions of compounds (**1a**–**6a**) & fluconazole with heme iron in the CYP51 cavity.

Compd. no.	Interaction of the ligand at heme iron and amino acids[a] (within ~5 Å from the ligands molecular surface) in the CYP51 cavity	Distance of N_3 from heme iron (Å)	H-bond (Å)
1a	Both the pyrimidine N_3 and side chain NH are oriented close to the heme iron atom. The 4-fluorophenyl ring lies close for interaction with heme iron and the amino acids, that are in close vicinity of the molecule namely; TYR-116, PHE-110, ALA-115, LEU-127.	2.854	3.047 (NH with heme iron)
3a	The heme iron atom is close to the pyrimidine N_3. The side chain NH is oriented slightly away from the heme iron. The 4-fluorophenyl ring lies close for interaction with heme iron and the amino acids that are in close vicinity of the molecule namely; TYR-116, MET-123, PHE-110, ALA-115, ALA-117, LEU-127.	2.661	3.125 (NH with heme iron)
6a	Both the pyrimidine N_3 and side chain NH are oriented close to the heme iron atom. The 4-fluorophenyl ring also lies close for interaction with heme iron. It and the carbonyl −C═O of the ester group, interact with the amino acids, that are in close vicinity of the molecule namely; TYR-116, VAL-114, ALA-115, PHE-110, MET-123, LEU-127, MET-103, MET-106	2.824	4.981 (NH with heme iron)
Fluconazole	The N_4 of 1,2,4-triazole coordinates with the heme iron. The difluorophenyl ring lies close for interaction with heme iron and the amino acids that are in close vicinity of the molecule namely; TYR-103, MET-106, PHE-110, ALA-115, LEU-127, PHE-290, ALA-291, ALA-287.	2.392	–

[a] All amino acid mentioned are within ~5Å from the ligands molecular surface.

Table 4
CLogp values of rings fused to the pyrimidine scaffold.

Compound no.	**1a**	**3a**	**6a**	**4a**	**2a**	**6a**
Ring fused	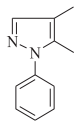	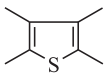	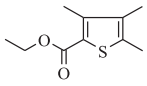	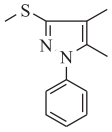	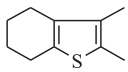	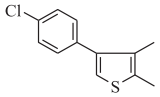
ClogP	2.684	3.364	3.760	3.332	4.308	5.045

*4.2.2. N-(4-Chlorophenyl)-1-phenyl-1H-pyrazolo[3,4-d]pyrimidin-4-amine (**1b**)*

Yield: 86.95%; mp 156–158 °C; IR (KBr): 3456 (N–H), 2917 (C–H), 1691 (N═N), 789 (C–Cl) cm^{-1}; ^1H NMR (300 MHz, $CDCl_3$) δ ppm: 7.18–7.45 (m, 4H, NH–Ar–*H*), 7.66–7.68 (s, 5H, N–Ar–*H*), 8.25 (s, 1H, N–N═C*H* at 5), 8.70 (s, 1H, N═C*H*–N at 2), 9.7 (s, 1H, N*H* at 4); ESI-MS *m*/*z*: 322 (M+1), 212, 195, 128. *Anal.* Calcd. for $C_{17}H_{12}ClN_5$ (321.76): C, 63.46; H, 3.76; N, 21.77. Found: C, 63.38; H, 3.52; N, 21.84.

*4.2.3. N-(3-Chloro-4-fluorophenyl)-1-phenyl-1H-pyrazolo[3,4-d] pyrimidin-4-amine (**1c**)*

Yield: 83.04%; mp 166–170 °C; IR (KBr): 3456 (N–H), 2937 (C–H), 1604 (C═N), 1556 (C═C), 731 (C–Cl) cm^{-1}; ^1H NMR (300 MHz, $CDCl_3$) δ ppm: 7.06–7.25 (m, 3H, NH–Ar–*H*), 7.72–7.75 (s, 5H, N–Ar–*H*), 8.08 (s, 1H, N–N═C*H* at 5), 8.55 (s, 1H, N═C*H*–N at 2), 9.44 (s, 1H, N*H* at 4); ESI-MS *m*/*z*: 340 (M+1), 212, 195, 146. *Anal.* Calcd. for $C_{17}H_{11}ClFN_5$ (339.75): C, 60.10; H, 3.26; N, 20.61. Found: C, 60.16; H, 3.18; N, 20.50.

*4.2.4. N-(4-Bromophenyl)-1-phenyl-1H-pyrazolo[3,4-d]pyrimidin-4-amine (**1d**)*

Yield: 81.05%; mp 168–172 °C; IR (KBr): 3428 (N–H), 2924 (C–H), 1601 (N═N), 780 (C–Br) cm^{-1}; ^1H NMR (300 MHz, $CDCl_3$) δ ppm: 7.40–7.66 (m, 4H, NH–Ar–*H*), 7.95–7.98 (s, 5H, N–Ar–*H*), 8.56 (s, 1H, N–N═C*H* at 5), 8.89 (s, 1H, N═C*H*–N at 2), 10.1 (s, 1H, N*H* at 4); ESI-MS *m*/*z*: 367 (M+1), 212, 195, 173. *Anal.* Calcd. for $C_{17}H_{12}BrN_5$ (366.21): C, 55.75; H, 3.30; N, 19.12. Found: C, 55.66; H, 3.22; N, 19.19.

*4.2.5. N-(Phenyl)-1-phenyl-1H-pyrazolo[3,4-d]pyrimidin-4-amine (**1e**)*

Yield: 80.55%; mp 180–184 °C; IR (KBr): 3452 (N–H), 2956 (C–H), 1536 (N═N) cm^{-1}; ^1H NMR (300 MHz, $CDCl_3$) δ ppm: 7.15–

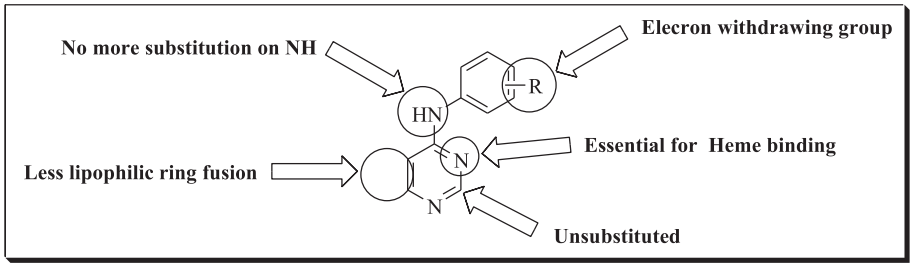

Fig. 11. Key structural requirement of condensed pyrimidine for antifungal activity.

7.35 (m, 5H, NH–Ar–*H*), 7.54–7.56 (s, 5H, N–Ar–*H*), 7.99 (s, 1H, N–N=C*H* at 5), 8.26 (s, 1H, N=C*H*–N at 2), 9.0 (s, 1H, N*H* at 4); ESI-MS *m/z*: 288 (M+1), 212, 195, 94. *Anal.* Calcd. for $C_{17}H_{13}N_5$ (287.32): C, 71.06; H, 4.56; N, 24.37. Found: C, 71.22; H, 4.37; N, 24.26.

*4.2.6. 2H-4-Fluorophenyl-(5,6,7,8-tetrahydrobenzo(b)thieno[2,3-d] pyrimidin-4-yl)-amine (**2a**)*

Yield: 86.95%; mp 166–168 °C; IR (KBr): 3432 (N–H), 2924 (C–H), 1560 (N=N), 828 (C–F) cm^{-1}; ^1H NMR (300 MHz, $CDCl_3$) δ ppm: 1.83 (s, 4H, CH_2 at 6 & 7), 2.60 (s, 4H, CH_2 at 5&8), 6.89–7.25 (m, 4H, NH–Ar–*H*), 8.1 (s, 1H, C*H* at 2), 8.8 (s, 1H, N*H* at 4); ESI-MS *m/z*: 300 (M+1), 206, 189, 112. *Anal.* Calcd. for $C_{16}H_{14}FN_3S$ (299.37): C, 64.19; H, 4.71; N, 14.04; S, 10.71. Found: C, 64.26; H, 4.63; N, 14.19; S, 10.88.

*4.2.7. 2H-(4-Fluorophenyl)-(5,6-dimethylthieno[2,3-d]pyrimidin-4-yl)-amine (**3a**)*

Yield: 86.31%; mp 166–170 °C; IR (KBr): 3427 (N–H), 2917 (C–H), 1602 (N=N), 900 (C–F) cm^{-1}; ^1H NMR (300 MHz, $CDCl_3$) δ ppm: 1.95 (s, 3H, CH_3 at 6), 2.22 (s, 3H, CH_3 at 7), 7.05–7.33 (m, 4H, NH–Ar–*H*), 8.15 (s, 1H, *CH* at 2), 8.77 (s, 1H, N*H* at 4); ESI-MS *m/z*: 274 (M+1), 180, 163, 112. *Anal.* Calcd. for $C_{14}H_{12}FN_3S$ (273.33): C, 61.52; H, 4.43; N, 15.37; S, 11.73. Found: C, 61.33; H, 4.50; N, 15.47; S, 11.80.

*4.2.8. N-(4-Flurophenyl)-3-(methylthio)-1-phenyl-1H-pyrazolo [3,4-d]pyrimidin-4-amine (**4a**)*

Yield: 89.10%; mp 152–156 °C; IR (KBr): 3306 (N–H), 2916 (C–H), 1590 (N=N), 987 (C–F) cm^{-1}; ^1H NMR (300 MHz, $CDCl_3$) δ ppm: 2.45 (s, 3H, S–CH_3 at 5), 6.88–7.25 (m, 4H, NH–Ar–*H*), 7.63–7.66 (s, 5H, N–Ar–*H*), 8.5 (s, 1H, N=C*H*–N at 2), 9.1 (s, 1H, N*H* at 4); ESI-MS *m/z*: 352 (M+1), 258, 241, 112. *Anal.* Calcd. for $C_{18}H_{14}FN_5S$ (351.4): C, 61.52; H, 4.02; N, 19.93; S, 9.12. Found: C, 61.36; H, 4.15; N, 20.05; S, 9.17.

*4.2.9. (4-Fluorophenyl)-[5-(4-chlorophenyl)thieno[2,3-d] pyrimidin-4-yl]-amine (**5a**)*

Yield: 91.85%; mp 185–188 °C; IR (KBr): 3408 (N–H), 1352 (C–F) cm^{-1}; ^1H NMR (300 MHz, $CDCl_3$) δ ppm: 6.15 (s, 1H, *CH* at 6), 7.07–7.42 (m, 4H, m, NH–Ar–*H*), 7.78–8.10 (m, 4H, Ar–*H* at 5), 8.63 (s, 1H, N=C*H*–N at 2), 9.0 (s, 1H, N*H* at 4); ESI-MS *m/z*: 356 (M+1), 262, 245, 112. *Anal.* Calcd. for $C_{18}H_{11}ClFN_3S$ (355.82): C, 60.76; H, 3.12; N, 11.81; S, 9.01. Found: C, 60.68; H, 3.02; N, 11.63; S, 9.19.

*4.2.10. 4-(4-Fluorophenylamino)-5-methylthieno[2,3-d]pyrimidin-6-carboxylate (**6a**)*

Yield: 88.51%; mp 182–185 °C; IR (KBr): 3173 (N–H), 2926 (C–H), 1689 (C=O), 1372 (C–F) cm^{-1}; ^1H NMR (300 MHz, $CDCl_3$) δ ppm: 1.25–1.61 (t, 3H, $COOCH_2CH_3$ at 6), 2.96–2.98 (s, 3H, CH_3 at 5), 4.37–4.42 (m, 2H, $COOCH_2CH_3$ at 5), 7.11–7.38 (m, 4H, m, NH–Ar–*H*), 8.07 (s, 1H, N=C*H*–N at 2), 8.88 (s, 1H, N*H* at 4); ESI-MS *m/z*: 332 (M+1), 286, 238, 221, 112. *Anal.* Calcd. for: $C_{16}H_{14}FN_3O_2S$ (331.36): C, 57.99; H, 4.26; N, 12.68; S, 9.68. Found: C, 57.84; H, 4.20; N, 12.47; S, 9.61.

4.3. Determination of antifungal activity

All the target compounds were tested against three pathogenic fungal strains *Candida albicans* (ATCC®90028), *Aspergillus fumigatus* (ATCC®204305) & *Aspergillus niger* (ATCC®9142) for their inhibitory activity, using a Mueller-Hinton broth by serial dilution method in 96 multicell microlitre plates in duplicate. All these organisms were procured from ATCC, LGC Promochem Pvt., Bangalore, India. The control strains of same organisms were also developed in suitable culture media. The inoculums of both, the control strains and clinical isolates were standardized by adjusting to McFareld scale (0.5) using Mueller-Hinton broth (10^5 CFU/ml). Antifungal activity was examined by the disc diffusion method under standard conditions using potato-dextrose agar (according to CLSI guidelines) [17]. Sterile filter paper discs (5 mm diameter, Whatman no. 3 chromatography paper) were dripped with compound solutions (DMSO) to load 500 mg of a given compound per disc. Dry discs were placed on the surface of appropriate agar medium. The results were read after 30 h of incubation at 36 °C. Compounds which showed activity in disc diffusion tests were examined by the agar dilution method to determine their MIC's minimal inhibitory concentration (CLSI) [18].

The MIC's of the compounds were studied by disc diffusion method making serial dilution of the compounds from the range 2–2048 μg/ml. The optical densities of spores in 0.2% tween 80 solutions were adjusted to 50 at 540 nm using a colorimeter.

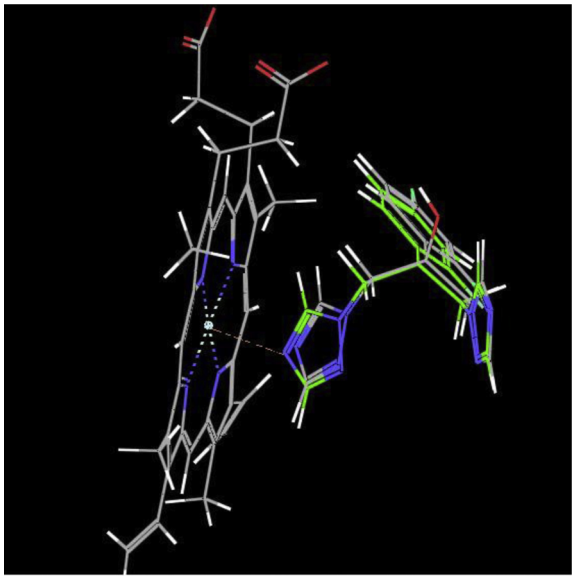

Fig. 12. Overlay of the best docked conformation of fluconazole over the X-ray structure in presence of heme.

4.4. Docking studies

All the molecular modelling studies were carried out on Intel Xeon based system with the Linux Enterprise OS using the Schrödinger molecular modelling package (Schrödinger, Inc., USA).

4.4.1. Molecular docking

Molecular docking studies were performed using the Glide module incorporated in the Schrödinger molecular modelling package. Glide Extra-Precision (XP) scoring function was adopted in the current study to estimate protein-ligand binding affinities. This scoring function is equipped with force field-based parameters accounting for solvation and repulsive interactions, lipophilic, hydrogen bonding interactions, metal-ligand interactions as well as contributions from coulombic and van der Waals interaction energies, all incorporated in the empirical energy functions.

4.4.2. Preparation of protein and ligand structures for docking simulations

The X-ray structure of sterol 14α-demethylase (CYP51) in complex with inhibitor fluconazole (PDB code: 3KHM) [19] was obtained from the RCSB Protein Data Bank (PDB), http://www.rcsb.org/pdb. The protein-inhibitor complex was prepared for Glide calculations by running the protein preparation wizard applying

the OPLS-2005 force field. Any crystallographic water, if present was eliminated and hydrogens were added to the structure corresponding to pH 7.0 considering the appropriate ionization states for both the acidic and basic amino acid residues. After assigning appropriate charge and protonation state, prepared structure was subjected to energy minimization until the average root mean square deviation (r.m.s.d.) reached 0.3Å.

The 3D structures of the condensed 2*H*-4-arylaminopyrimidines were built in the Maestro Suite of the module and subsequently optimized using the *LigPrep* module in the Schrödinger Suite. Partial atomic charges were computed using the OPLS-2005 force-field and possible ionization states were generated at a pH of 7.0. The ligand structures thus obtained were further optimized by energy minimization using the LBFGS method until a gradient of 0.01 kcal/mol/Å was achieved. These optimized protein and ligand geometries were used as input for the docking study.

4.4.3. Receptor Grid Generation

After ensuring that the protein and ligands were in the correct form, the receptor-grid was generated to define the active site for docking using the *Receptor Grid Generation* tool in Glide. With the non-covalently bound native ligand fluconazole in place, grid file was generated using the co-crystallized ligand at the centre of the two boxes. The binding site was defined by a 10Å × 10Å × 10Å box centred on the centroid of fluconazole in the crystal complex so as to explore a large portion of the protein.

For the precision and accuracy of the docking protocol the co-crystallised ligand (fluconazole) was extracted from this crystal structure and re-docked using the Glide docking algorithm in the XP mode. A good agreement was observed between the localization of the fluconazole upon docking and from the crystal structure as is evident from a low rmsd of less than 1.0Å. Hence, the reliability of the Glide docking procedure for predicting binding modes of other molecules in the dataset was confirmed. The best scoring pose for fluconazole obtained by docking has been compared against the crystal structure in Fig. 12.

Based on our earlier results on anticancer activity in 2*H*-4-(substituted)phenylamino-pyrazolopyrimidines, two of the derivatives **1a** & **1b** which have also shown good antimicrobial activity, were first envisaged for the docking study and based on the results of this study, subsequent synthesis and antifungal evaluation of some more related derivatives was planned. With the receptor grid generated for fluconazole in the validation study, fluconazole and the above two inhibitors (**1a** & **1b**), were subjected to flexible docking. For each compound 10 poses with the best Glide Scores were saved and analyzed for the key elements of interaction with the receptor.

Acknowledgements

The authors acknowledge Sinhgad Technical Education Society, Pune, India and Department of Chemistry, University of Pune, India for providing facilities to carry out the synthetic work and spectroscopic analysis, and Principal, Bombay College of Pharmacy, Mumbai, India for providing facilities to carry out *in silico* experiments.

Appendix A. Supplementary data

Supplementary data related to this article can be found at http://dx.doi.org/10.1016/j.ejmech.2014.02.066.

References

[1] (a) A. Amorim, L.G. Vacz, R. Aanjo, International Journal of Antimicrobial Agents 3 (2010) 396–399;
(b) E. Giavini, E. Menegola, Toxicology Letters 198 (2010) 106–111;
(c) S.K. Funkin, W.R. Jarvis, Clinical Microbiology Reviews 9 (1996) 499–511;
(d) J.R. Wingard, H. Leather, Biology of Blood and Marrow Transplantation 10 (2001) 73–90;
(e) N.H. Georgopapdakou, T.J. Walsh, Antimicrobial Agents and Chemotherapy 6 (1996) 279–291;
(f) J.N. Steenbergen, A. Casadevall, Journal of Clinical Microbiology 38 (2000) 1974–1976.
[2] (a) O. Kniemeyer, A.D. Schmidt, M. Vadisch, D. Wartenberg, A.A. Brelgage, International Journal of Medical Microbiology 301 (2011) 368–377;
(b) K.A. Marr, Oncology 18 (2004) 9–14;
(c) P. Gastmeier, Journal of Hospital Infection 63 (2000) 246–254.
[3] Z. Bhatti, A. Shukat, N.G. Almyroudis, B.H. Segal, Mycopathologia 162 (2006) 1–15.
[4] C.B. Moore, N. Sayers, J. Mosquera, J. Slaven, D.W. Denning, Journal of Infection 41 (2000) 203–220.
[5] P. Bowyer, C.B. Moore, R. Rautemaa, D.W. Denning, M.D. Richardson, Current Infectious Disease Reports (2011), http://dx.doi.org/10.1007/s11908-011-0218-4.
[6] J. Xu, Y. Cao, J. Zhang, S. Yu, Y. Zou, X. Chai, Q. Wu, D. Zhang, Y. Jiang, Q. Sun, European Journal of Medicinal Chemistry 46 (2011) 3142–3148.
[7] (a) J.M. Beale Jr., J.H. Block (Eds.), Wilson & Gisvold's Text Book of Organic Medicinal & Pharmaceutical Chemistry, Antiinfective Agents, Wolter Kluwer-Lippincott Williams & Wilkins, New Delhi, 2011, pp. 179–241;
(b) X. Chai, J. Zhang, H. Hu, S. Yu, Q. Sun, Z. Dan, Y. Jiang, Q. Wu, European Journal of Medicinal Chemistry 46 (2011) 3142–3148.
[8] P.D. Patel, M.R. Patel, B. Kocsis, E. Kocsis, S.M. Graham, A.R. Warren, S.M. Nicholson, B. Billack, F.R. Fronczek, T.T. Talele, European Journal of Medicinal Chemistry 45 (2010) 2214–2222.
[9] K.S. Jain, T.S. Chitre, P.B. Miniyar, M.K. Kathiravan, V.S. Bendre, V.S. Veer, S.R. Shahane, C.J. Shishoo, Current Science 90 (6) (2006) 793–803.
[10] C.J. Shishoo, M.B. Devani, V.S. Bhadti, Indian Pat. (1981) 151 496; Chem. Abstr., 1984, 100 209858.
[11] C.J. Shishoo, T.R. Gandhi, I.S. Rathod, K.S. Jain, R.K. Goyal, Arzneimittel-Forschung Drug Research 47 (1997) 1125–1129.
[12] C.J. Shishoo, K.S. Jain, I.S. Rathod, B.J. Thakkar, S.B. Brahmabhatt, T.P. Gandhi, R. Bangaru, R.K. Goyal, Arzneimittel-Forschung Drug Research 46 (1996) 273–276.
[13] (a) M.K. Kathiravan, C.J. Shishoo, K.G. Kumar, S.K. Roy, K.R. Mahadik, S.S. Kadam, K.S. Jain, Arzneimittel-Forschung Drug Research 57 (9) (2007) 599–606;
(b) M.K. Kathiravan, K.D. More, V.K. Raskar, K.S. Jain, M. Maheshwar, S. Gadhwe, D.P. Jain, M.A. Nagras, Medicinal Chemistry Research 22 (2013) 4286–4292.
[14] (a) M.S. Phoujdar, J.B. Bariwal, A.K. Shah, M.K. Kathiravan, R.S. Somani, J.R. Jagtap, K.S. Jain, International Journal of Pharmaceutical Sciences and Research 42 (3) (2008) 222–228;
(b) P.B. Dudhe, K.S. Jain, V.K. Raskar, A.S. Deodhe, J.G. Patel, M.K. Kathiravan, Medicinal Chemistry Research 22 (2013) 3719–3727.
[15] K.S. Jain, M.N. Navale, Indian Pat. Appln. (730/MUM/2012, dated 19 March 2012).
[16] K.S. Jain, M.K. Kathiravan, J.B. Bariwal, P.K. Chaskar, S.S. Tompe, N. Arya, Synthetic Communications 43 (5) (2013) 719–727.
[17] (a) J.L. Beebe, E.W. Koneman, Clinical Microbiology Reviews 8 (1995) 336;
(b) Clinical and Laboratory Standards Institute, "Method for Antifungal Disk Diffusion Susceptibility Testing of Yeasts; Approved Standard M44; Clinical and Laboratory Standards Institute," Wayne, Pa, USA, 2006.
[18] (a) B.A. Adeniyi, H.H.S. Fong, J.M. Pezzuto, L. Luyengi, H.A. Odelola, Phytotherapy Research 14 (2000) 112–117;
(b) O.O. Aiyelaagbe, E.K. Adesogan, O. Ekundayo, B.A. Adeniyi, Phytotherapy Research 14 (2000) 60–62;
(c) Clinical and Laboratory Standards Institute, "Reference Method for Broth Dilution Antifungal Susceptibility Testing of Yeasts; Approved Standard M27; Clinical and Laboratory Standards Institute," Wayne, Pa, USA, 2006.
[19] G.I. Lepesheva, T.Y. Hargrove, S. Anderson, Y. Kleshchenko, V. Furtak, Z. Wawrzak, F. Villalta, M.R. Waterman, Journal of Biological Chemistry 285 (33) (2010) 25582–25590.